

Diffusion behavior of implanted Li ions in GaN thin films studied by secondary ion mass spectrometry

F. Salman^a, L. Chow^{a,*}, B. Chai^b, F.A. Stevie^c

^a*Department of Physics, University of Central Florida, Orlando, FL 32816, USA*

^b*Crystal Photonics, Inc., 5525 Benchmark Lane, Sanford, FL 32773, USA*

^c*Analytical Instrumentation Facility, North Carolina State University, Raleigh, NC 27695, USA*

Available online 17 February 2006

Abstract

Lithium ions with dosages of 2.6×10^{12} , 2.6×10^{13} , 2.6×10^{14} , and $2.6 \times 10^{15} \text{ cm}^{-2}$ have been implanted into a GaN thin film grown on sapphire substrates. The diffusion behavior of these implanted Li ions in GaN thin film at different temperature anneals was studied using secondary ion mass spectrometry. In general, the diffusion profiles show relatively little movement of Li in the GaN thin film for temperatures up to 700 °C. At low-temperature anneals (<500 °C), up-hill diffusion dominated the Li profiles and at high-temperature anneals (>800 °C), out-diffusion dominated the Li profiles. © 2006 Elsevier Ltd. All rights reserved.

Keywords: GaN; Diffusion; SIMS

1. Introduction

Nitride-based semiconductor products have excited considerable interest in the last several years because of their potential for applications in optoelectronics and in high-power and high-frequency electronic devices [1]. The fact that GaN has a wide and direct band gap (3.39 eV at room temperature) makes GaN an excellent candidate material for short-wavelength optical devices, especially for blue, green, violet, and ultraviolet (UV) light-emitting diodes (LEDs), and blue laser diodes (LDs) [2–5]. For the fabrication of these optical devices, a high-quality GaN thin film is required [6]. Many GaN devices are based on GaN thin films grown on substrates such as sapphire. Devices

grown on SiC or Si substrates typically use AlGaIn as a transition material to reduce lattice mismatch. Sapphire (0001) has been used as a substrate for GaN thin film growth [7,8] because of ready availability. However, it is difficult to grow high-quality GaN thin films on a sapphire substrate with smooth surfaces because of the mismatch in lattice constants and thermal expansion coefficients between GaN and sapphire [2,9]. Therefore, there is a need to replace sapphire for the direct growth of high-quality GaN devices. Hellman et al. [10] in 1997 were the first to discuss the possibility of growing GaN on γ -LiAlO₂. The (10 $\bar{1}$ 0) plane of GaN is closely lattice matched with the (100) plane of LiAlO₂. In 2000, Waltereit et al. [11] have grown (10 $\bar{1}$ 0)-oriented GaN films by molecular beam epitaxy (MBE) on (100) γ -LiAlO₂ substrates.

Recently, Maruska et al. [8] reported the growth of thick films of GaN (300–400 μm) on γ -LiAlO₂ substrates. They found high concentrations of Li

*Corresponding author. Tel.: +1 407 823 2333;
fax: +1 407 823 5112.

E-mail address: chow@ucf.edu (L. Chow).

and Al on the rear surface of the GaN thin film indicating the diffusion of Li and Al ions from the γ -LiAlO₂ substrate into the GaN film during growth. A typical secondary ion mass spectrometry (SIMS) depth profile of the rear surface of a GaN film grown on γ -LiAlO₂ is shown in Fig. 1. It can be seen that very high concentrations of Li and Al are present within the first 0.5 μm below the surface of the rear side of the GaN film.

Information is lacking for diffusion data of Li in GaN. Wilson et al. [12] examined the thermal stability of eight different dopants implanted into GaN thin films. They found that for Be, C, Mg, Si, Zn, and Ge, the implanted dopant profiles do not change after 800 °C anneal. For S or Se it was found that their profiles started to redistribute after 600 or 800 °C anneal respectively. The location of the ion-implanted Li in GaN has been studied by Dalmer et al. [13]. They showed that the ion-implanted Li mainly occupied interstitial sites in the center of the *c*-axis hexagons at positions *c*/4 and 3*c*/4. This result agreed with the well-known knowledge that Li is a fast interstitial diffuser in most semiconductors.

To better understand the diffusion of Li ions in GaN, we outlined a program to implant different dosages of Li ions into a GaN thin film grown on sapphire substrate. These implanted samples would be annealed at several temperatures between 300 and 1000 °C and the re-distribution of Li ions after annealing studied using SIMS [14–16].

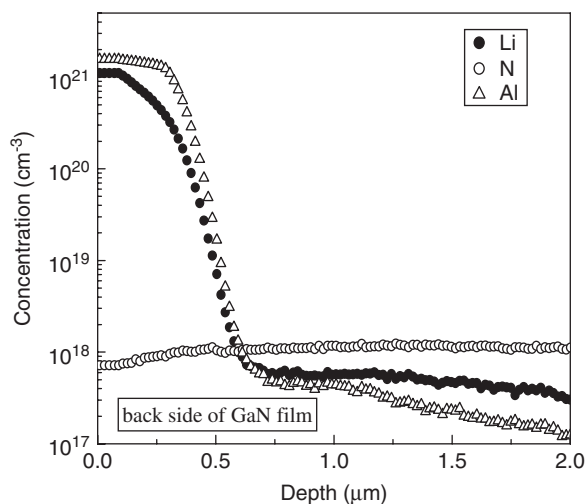


Fig. 1. SIMS depth profiles of Li, N and Al in the backside of a GaN thin film grown on γ -LiAlO₂ substrate.

2. Experiment

The GaN thin film was grown on a 2.0" diameter sapphire wafer using a halide vapor phase epitaxy system [8] at Crystal Photonics. After deposition, the wafer was divided into 4 pieces that were separately ion implanted with Li ions to dosages of 2.6×10^{12} , 2.6×10^{13} , 2.6×10^{14} , and $2.6 \times 10^{15} \text{ cm}^{-2}$. The implantation was carried out at room temperature with an implantation energy of 90 keV. Thermal anneals were performed for the implanted samples in the temperature range 300–1000 °C for 30 min each. The annealing processes were carried out in a Lindberg furnace using a long quartz tube. Once the desired temperature was reached, the quartz tube with the sample was placed into the center of the furnace. The annealing temperature was controlled to within ± 1 °C. A constant flow of high-purity (99.999%) argon gas was maintained through the quartz tube throughout the annealing process. After completion of the annealing process, the quartz tube was removed from the furnace and the samples were cooled to room temperature in an argon environment.

SIMS was used to obtain depth profiles of the Li dopants. The SIMS characterization was conducted at the UCF/Agere Materials Characterization Facility with a CAMECA IMS-3f using O₂⁺ primary beam at 100 nA measured using a Faraday cup. An impact energy of 5.5 keV, and an impact angle of 40° from normal were typical parameters used in our SIMS measurements. The focused primary beam of oxygen ions was rastered over 200 × 200 or 250 × 250 μm^2 areas, with detection of ions from an area of 60 μm diameter at the center of the raster. The sputtering rate was approximately 0.6 nm/s. The depth scale was established for each profile by measuring the crater depth with a stylus profilometer (Sloan Dektak IIA). The concentration was calibrated with the implantation dosages of the as-implanted samples and the measured erosion rate.

3. Results and discussion

Figs. 2 to 6 present the results of the Li diffusion analyses. Fig. 2 shows the depth profiles of the as-implanted Li ions at four different dosages. At $2.6 \times 10^{12} \text{ cm}^{-2}$ dosage, the Li concentration at the surface of the film is about $2 \times 10^{16} \text{ cm}^{-3}$ and gradually increased to a maximum of $9 \times 10^{16} \text{ cm}^{-3}$ at a depth of 0.38 μm . The Li concentration then drops to $\approx 10^{14} \text{ cm}^{-3}$ at a depth of 1.5 μm . At

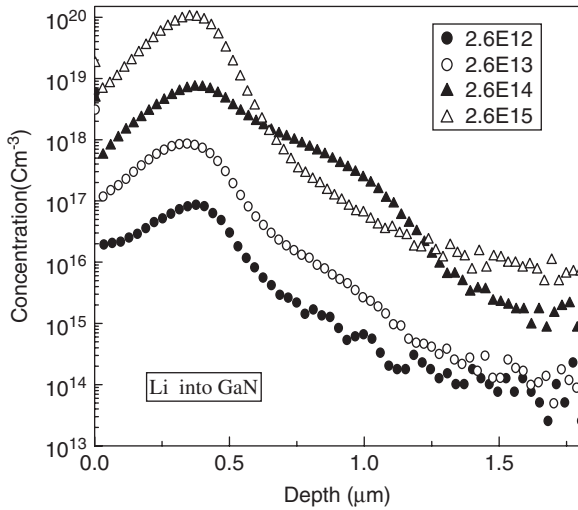


Fig. 2. SIMS depth profiles of several dosages of Li ions implanted into a GaN film grown on sapphire substrate. (2.6×10^{12} , 2.6×10^{13} , 2.6×10^{14} , and 2.6×10^{15} atoms/ cm^2).

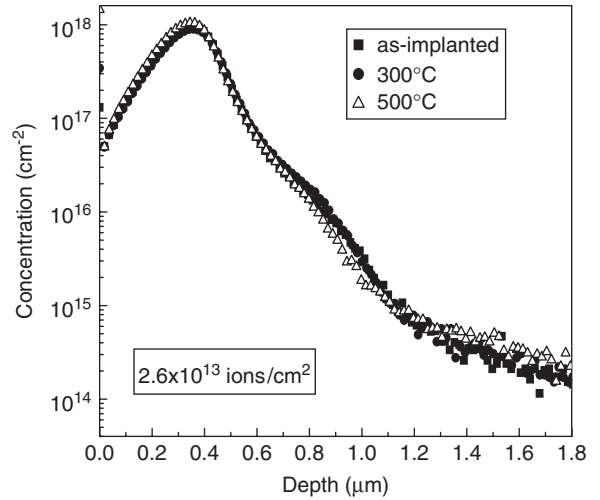


Fig. 4. SIMS depth profiles of Li 2.6×10^{13} atoms/ cm^2 into GaN thin film for as-implanted and annealed samples.

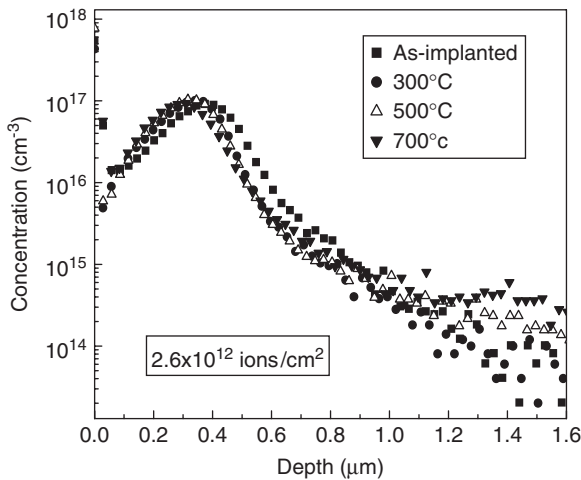


Fig. 3. SIMS depth profiles of Li 2.6×10^{12} atoms/ cm^2 into GaN thin film for as-implanted and annealed samples.

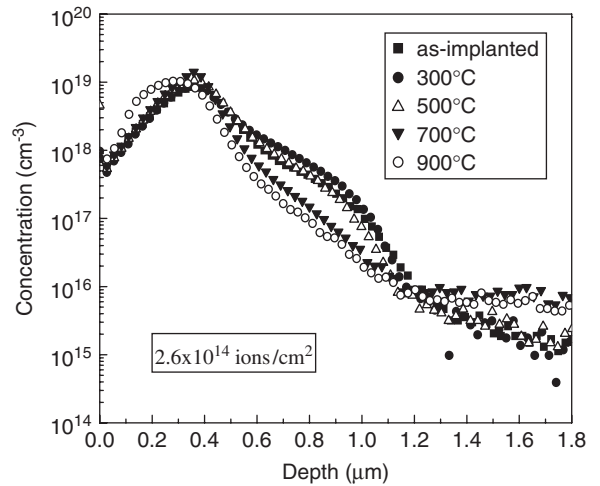


Fig. 5. SIMS depth profiles of Li 2.6×10^{14} atoms/ cm^2 into GaN thin film for as-implanted and annealed samples.

$2.6 \times 10^{13} \text{ cm}^{-2}$ dosage, the shape of Li distribution is very similar to the result from a $2.6 \times 10^{12} \text{ cm}^{-2}$ implant, but the magnitude remains at $0.38 \mu\text{m}$ below the surface and the peak concentration is about $9 \times 10^{17} \text{ cm}^{-3}$. As we go deeper into the film, the Li concentration gradually drops to $\approx 10^{14} \text{ cm}^{-3}$ at a depth of $1.5 \mu\text{m}$, which is the same as that at $2.6 \times 10^{12} \text{ cm}^{-2}$ dosage. This value of 10^{14} cm^{-3} Li concentration represents the detection limit of Li ions for our instrument.

At $2.6 \times 10^{14} \text{ cm}^{-2}$ dosage, the shape of the as-implanted Li ion distribution in GaN is very different

from that at other dosages. For example, the full-width at half-maximum (FWHM) is clearly wider than the widths at the other three dosages. In addition, there exists a clear “shoulder” (or “bump”) at depth between 0.7 and $1.3 \mu\text{m}$. We noticed that the Li concentration in this “shoulder” is even higher than that due to the implant at $2.6 \times 10^{15} \text{ cm}^{-2}$ dosage. The Li concentration eventually drops to $1 \times 10^{15} \text{ cm}^{-3}$ at a depth of $1.5 \mu\text{m}$.

At $2.6 \times 10^{15} \text{ cm}^{-2}$ dosage, the shape of the Li distribution follows the Li profiles obtained at 2.6×10^{12} and $2.6 \times 10^{13} \text{ cm}^{-2}$ dosages. At this high

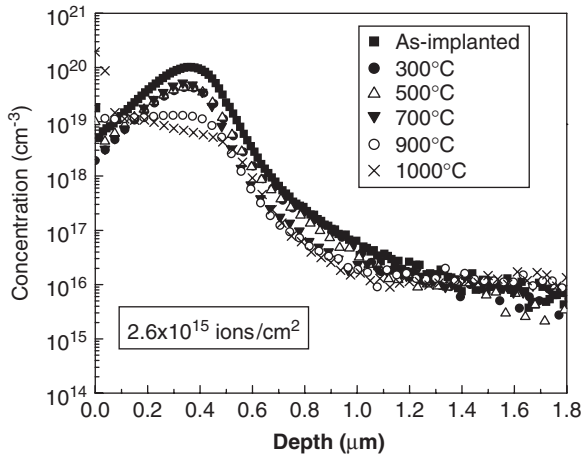


Fig. 6. SIMS depth profiles of Li 2.6×10^{15} atoms/cm² into GaN thin film for as-implanted and annealed samples.

dosage, the Li background concentration at a depth of $1.5 \mu\text{m}$ is about $1 \times 10^{16} \text{cm}^{-3}$, which is about two orders of magnitude higher than the Li background concentrations at the same depth but at lower dosages.

It is not clear why the Li distribution at $2.6 \times 10^{14} \text{cm}^{-2}$ dosage is different from the Li distributions at other dosages. One plausible explanation would be that there was a channeling effect during that particular implant that results in a deeper penetration of the Li ions and a broader FWHM.

Fig. 3 shows the Li profiles in GaN at dosage $2.6 \times 10^{12} \text{cm}^{-2}$ as-implanted and annealed at 300, 500, and 700 °C. There were two unusual features worth noticing. One was the uphill diffusion of Li in GaN. At 300 °C anneal, the peak position of the Li distribution moved $0.04 \mu\text{m}$ toward the surface. This movement increased to $0.06 \mu\text{m}$ at 500 °C anneal, and $0.08 \mu\text{m}$ at 700 °C. This type of uphill diffusion has been observed in a profile of implanted and annealed Mg in GaAs [17]. The other unusual feature of the Li profiles in Fig. 3 is the out-diffusion of Li ions near the surface. The out-diffusion of implanted Be in GaAs has been studied before [18]. This out-diffusion of Li ions generated a high Li concentration near the surface. The two main reasons for this behavior could be: (a) surface damage acted as a sink for the Li ions and (b) the low solubility of the Li ion in GaN.

Fig. 4 shows the Li profiles of implanted Li ions at $2.6 \times 10^{13} \text{cm}^{-2}$ as-implanted and annealed at 300 and 500 °C. The size of the sample at this dosage

was quite small, therefore we only annealed at two different temperatures. Our results indicated that Li profiles seem to remain almost unchanged after 300 and 500 °C anneals. The only minor change in the concentration occurred in the depth range from 0.6 to $1.0 \mu\text{m}$.

Fig. 5 shows the Li profiles of implanted Li ions at $2.6 \times 10^{14} \text{cm}^{-2}$ as-implanted and annealed at 300, 500, 700 and 900 °C. At 300 °C anneal, the diffusion behavior is very similar to the diffusion behavior in Fig. 4, i.e. the profile remained the same except for an increase in Li ions in the depth range of 0.6 to $1.0 \mu\text{m}$. At 500 °C anneal, the Li ions distribution almost remained unchanged. As the anneal temperatures increased the Li diffusion behavior was very similar to that at lower dosages. In particular, the up-hill diffusion of Li ions can be seen very clearly. The Li peak concentration actually increased [17] and the FWHM decreased after 700 °C anneal. At 900 °C anneal, the Li concentration peak moved toward the surface. We also noticed some Li in-diffusion at a depth of $1.8 \mu\text{m}$, i.e. as-implanted and low-temperature anneals ($< 600 \text{ °C}$) showed a Li concentration of $2 \times 10^{15} \text{cm}^{-3}$ at $1.8 \mu\text{m}$, while for the high temperature anneals ($> 600 \text{ °C}$), the Li background increased five-fold to $1 \times 10^{16} \text{cm}^{-3}$ at the same depth.

At our highest implant dosage, $2.6 \times 10^{15} \text{cm}^{-2}$, the Li diffusion behavior is dominated by out-diffusion at high-temperature anneals ($> 800 \text{ °C}$) as shown in Fig. 6. After 900 °C anneal, the Li distribution becomes almost constant at $1 \times 10^{19} \text{cm}^{-3}$ from a depth of 20 to 400 nm below the surface. Near the surface the Li concentration increased to $1 \times 10^{21} \text{cm}^{-3}$. The Li profiles beyond the projected range inside the GaN ($0.5\text{--}1.2 \mu\text{m}$) showed some up-hill diffusion such that the Li concentration in this region decreased after high-temperature anneals. The Li background concentration at $1.8 \mu\text{m}$ changed from $5 \times 10^{15} \text{cm}^{-3}$ at low-temperature anneals to $1 \times 10^{16} \text{cm}^{-3}$ after high-temperature anneals. This may be due to the high peak concentration of Li in this sample. There is a limit to dynamic range of $10^4\text{--}10^5$ because of resputtering events from the cover plate immediately in front of the first lens (immersion lens).

4. Summary

From our experimental studies, we have shown that the concentration profiles of implanted Li ions in GaN thin films are dependent on the

implantation dosages and the annealing temperatures. These concentration profiles reflect the complexity of the interactions between the defects and the implants. But from another point of view, our data also showed that in general, except for the highest dosages and anneal temperatures, there is *relatively* little movement of Li in the GaN thin film. We also demonstrated that SIMS was able to provide the sensitivity and depth resolution to study the as-implanted and annealed Li distributions in GaN thin films.

Acknowledgments

Lee Chow and Fatma Salman wish to acknowledge the financial support from Crystal Photonics, Inc. and technical support from UCF /Agere Materials Characterization Facility (MCF).

References

- [1] Nakamura S, Fasol G. The blue laser diode-gallium-nitride based light emitters and laser. New York: Springer; 1997.
- [2] Morkoc H, Strite S, Gao GB, Lin ME, Sverdlov B, Burns M. J Appl Phys 1994;76:1363.
- [3] Lester SD, Ponce FA, Craford MG, Steigerwald DA. Appl Phys Lett 1995;66:1249.
- [4] Nakamura S, Senoh M, Nagahama SI, Iwasa N, Yamada T, Matsushita T, et al. Appl Phys Lett 1996;68:2105.
- [5] Aktas O, Kim W, Fan Z, Bothkarev A, Salvador A, Mohammad SN, et al. Electron Lett 1995;31:1389.
- [6] Nakamura S, Harada Y, Senoh M. Appl Phys Lett 1991;58:2021.
- [7] Maruska HP, Tietjen JJ. Appl Phys Lett 1969;15:327.
- [8] Maruska HP, Hill DW, Chou MC, Gallagher JJ, Chai BH. Opto-Electron Rev 2003;11:7.
- [9] Amano H, Hiramatsu K, Akasaki I. Jpn J Appl Phys 1988;27:L1384.
- [10] Hellman ES, Liliental-Weber Z, Buchanan DNE. MRS Internet J Nitride Semicond Res 1997;2:30.
- [11] Waltereit P, Brandt O, Ramsteiner M, Trampert A, Grahn HT, Menniger J, et al. Phys Status Solidi A 2000;180:133.
- [12] Wilson RG, Pearton SJ, Abernathy CR, Zavada JM. Appl Phys Lett 1995;66(17):2238.
- [13] Dalmer M, Restle M, Vetter U, Hofsass H, Bremser MD, Ronning C, et al. J Appl Phys 1998;84:3085.
- [14] Francois-Saint-Cyr HG, Anoshkina E, Stevie F, Chow L, Richardson K, Zhou D. J Vac Sci Technol B 2001;19:1769.
- [15] Francois-Saint-Cyr HG, Stevie F, McKinley JM, Elshot K, Chow L, Richardson K. J Appl Phys 2003;94(12):7433.
- [16] Zhang P, Stevie F, Vanfleet R, Neelakantan R, Klimov M, Zhou D, et al. J Appl Phys 2004;96(2):1053.
- [17] Robinson HG, Deal MD, Amaratunga G, Griffin PB, Stevenson DA, Plummer JD. J Appl Phys 1992;71(6):2615.
- [18] Baratte H, Sadana DK, de Souza JP, Hallali PE, Schad RG, Norcott M, et al. J Appl Phys 1990;67(10):6589.